Transactions of the Indian National Academy of Engineering (2022) 7:823–834
https://doi.org/10.1007/s41403-022-00331-5

ORIGINAL ARTICLE

Comparative Studies on Ignition Kinetics and Detonation Chemistry of Real Distillate Fuels

M. S. Karthikeyan Iyer[1] · Ashlesh Dahake[1] · Ajay V. Singh[1]

Received: 16 December 2021 / Accepted: 18 March 2022 / Published online: 13 April 2022

Abstract

The effect of ignition kinetics and fuel chemistry of conventional jet fuels like JP-8, Jet-A, and JP-5 on the detonation length and time scales was studied and compared for applications in detonation-based combustors. The numerical calculations were carried out over a range of initial conditions to evaluate critical detonation responses of interest of real distillate fuels for their application in detonation-based combustors. The effect of the addition of ignition promoters and inert diluents on the ignition kinetics of real distillate fuels was also computed and compared. Results show that the global detonation properties of the three jet fuels are approximately the same under comparable conditions. Also, the length and time scales of real distillate fuels have very small variations under varying initial conditions. Similarly, the addition of ignition promoters shows similar reductions in the chemical length and times scales. The increase in the detonation length and time scales with the addition of inert diluents is also similar for the three jet fuels. For all the cases tested so far, the detonation chemistry and the critical detonation parameters are found to be very close to each other for JP-8, Jet-A, and JP-5. In so far as the global detonation properties are concerned, the three jet fuels tested exhibit nearly the same chemical behaviors and global combustion properties. Additionally, the three jet fuels tested yield nearly the same composition and amounts of pyrolysis products under comparable conditions. It is found that the pyrolysis product distribution determines the global detonation properties of the original, multicomponent jet fuels.

Keywords Gaseous detonations · Real distillate fuels · Ignition delay time · Detonation-based engines · Ignition promoters

List of Symbols

Δ_i	Induction zone length (mm)
τ_i	Induction delay time (μs)
$\dot{\sigma}$	Thermicity
T_0	Initial temperature (K)
P_0	Initial pressure (atm)
a_0	Upstream speed of sound (m/s)
φ	Equivalence ratio
P_{CJ}	Post-detonation pressure (atm)
T_{CJ}	Post-detonation temperature (K)
M_{CJ}	CJ detonation Mach number
V_{CJ}	CJ detonation velocity (m/s)
P_{VN}	Post-shock pressure (atm)
T_{VN}	Post-shock temperature (K)

Subscripts

VN	Von Neumann state
CJ	Chapman–Jouguet state

Introduction

Detonation cycle engines have been proposed as a promising alternative to conventional gas turbine engines for quite some time now (Heiser and Pratt 2002; Kailasanath 2000; Lu and Braun 2014; Nicholls et al. 1966; Wolański 2013). Although these engines have been developed in various research laboratories across the world, the practical implementation of the same for aircraft engines is still under process. It is well known from past experiments and computations that the fuel composition plays an important role in the overall performance of the engine as different fuels tend to exhibit different combustion behaviors. The critical detonation parameters for various fuel types tend to follow a distinct trend in certain cases. Recently, due to the scarcity of fossil fuels, biofuels are being used as a suitable alternative (Demirbas 2008; Dahake and Singh 2022a, b; Rodionova

✉ Ajay V. Singh
ajayvs@iitk.ac.in

[1] Department of Aerospace Engineering, Indian Institute of Technology Kanpur, Kanpur 208016, India

et al. 2017). Till now, gaseous fuels, such as hydrogen, methane, ethylene, propane, etc., have been widely used in detonation experiments and numerical calculations due to their simple chemistry. It is of interest to investigate the detonating behavior of liquid hydrocarbon fuels that has received little consideration so far when compared to gaseous fuels. Real distillate fuels and biofuels fall under such category, and it is essential to evaluate the detonation chemistry of such fuels since it can provide a concrete understanding of the detonating behavior of real distillate fuels.

Earlier, Stamps and Tieszen (1991) investigated the influence of initial temperature and pressure on hydrogen–air-diluent detonations. In his classical work, Westbrook (1982) investigated the role of chemical kinetics of hydrocarbon oxidation in gaseous detonations. Similarly, the detonation cell sizes and induction delay times in hydrogen nitrous oxide-diluent mixtures were predicted by Mevel et al. (2008) using a detailed chemical kinetics model. Garikov et al. (2000) also presented a model for cell size prediction using a chemical kinetic approach. Recently, Zhang (2019) investigated the detonability limits in methane–hydrogen–oxygen mixtures and pointed out the dominant role of induction length in gaseous detonations. Crane et al. (2019) studied the hydrogen–oxygen-diluent mixtures in the presence of ozone where they provided meaningful insights into the relationship between detonation cell size and chemical length scales. Vasil'ev (2006) also reported the vital role of cell size in a multifront detonation wave. Recently, Kumar et al. (2021) studied the effect of the addition of ignition promoters in small amounts on the chemical length and time scales of hydrogen–air/oxygen detonating mixtures. They reported the significance of fuel sensitization for improving the detonability limits and ignition kinetics of fuel–air mixtures. Liang et al. (2019) also investigated the explosion limits of hydrogen–oxygen mixtures in the presence of ozone. Peng et al. (2018) experimentally investigated the ethylene–air rotating detonation waves in a hollow chamber with a Laval nozzle. Recently, NO*x* emissions from Jet-A–air and C1–air detonations have been reported by Iyer and Singh (2021) and Dahake and Singh (2021), respectively.

Though some investigations have been performed for liquid hydrocarbon fuels in detonating environments, the effect of fuel chemistry on detonation parameters needs to be investigated for real distillate fuels. In this paper, conventional jet fuels like A1 (JP-8), A2 (Jet-A), and A3 (JP-5) are considered, and critical detonation parameters are investigated for each fuel–air mixture over a range of initial conditions. The evaluated parameters are compared with each other to explore the possible differences/similarities in their detonation behavior. A1, A2, and A3 are multicomponent fuels and seem to behave a lot differently in their combustion behavior when compared to their surrogates. This is evident as surrogates cannot capture the combustion chemistry of real distillate fuels over a wide range of initial conditions (Wang et al. 2018). In the present analysis, the HyChem reaction model is used to model the detonation chemistry of conventional jet fuels since it has been thoroughly validated against the experimental data and is shown to predict the global combustion properties of conventional jet fuels very well including the laminar flame speed, extinction strain rates, and ignition delay time. In the present work, the ZND calculations are carried out for conventional jet fuels at varying initial conditions. Also, the effect of inert diluents and ignition promoters on fuel–air detonating mixtures is reported and their performance is compared. In the present study, we consider three conventional, petroleum-derived jet fuels: JP-8, Jet A, and JP-5, designated here as A1, A2, and A3, respectively. Key properties of the conventional jet fuels studied are listed in Table 1.

Figure 1 presents typical compositions of three jet fuels. A1, A2, and A3 primarily contain n-paraffins, iso-paraffins, cyclo-paraffins, and aromatics, as depicted in Fig. 1. The jet fuels considered here are quite similar in their chemical composition. The only notable difference is in the concentration of various constituents.

Computational Methodology

The ZND calculations in the present work were carried out by integrating CANTERA 2.4.0 with MATLAB and Python (Goodwin et al. 2018). To compute the relevant ZND parameters, the modified CalTech Shock and Detonation Toolbox was used (Browne et al. 2008; Kao and Shepherd 2008). HyChem model (Hybrid Chemistry) was used to define the combustion chemistry of A1, A2, and A3 fuels. The HyChem model expresses fuel pyrolysis and oxidation of the pyrolysis products in two separate submodels (Wang et al. 2018). The HyChem model combines an experimentally constrained fuel pyrolysis model with a detailed

Table 1 Key properties of real distillate fuels

Fuel	Average molecular weight (g/mol)	LHV (MJ/kg)	H/C ratio	Average formula	Model formula
A1 (JP-8)	151.9	43.2	2.00	$C_{10.8}H_{21.6}$	$C_{11}H_{22}$
A2 (Jet-A)	158.6	43.1	1.90	$C_{11.4}H_{21.7}$	$C_{11}H_{22}$
A3 (JP-5)	166.1	42.9	1.86	$C_{12.0}H_{22.3}$	$C_{12}H_{23}$

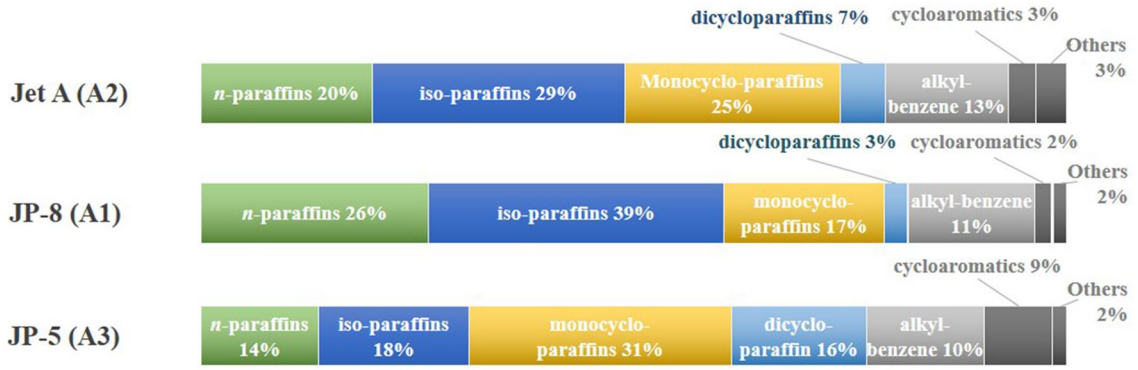

Fig. 1 Chemical composition of typical Jet-A (A2), JP-8 (A1), and JP-5 (A3) fuels

foundational fuel chemistry model for the oxidation of the pyrolysis products. In HyChem, USC Mech II is used as a foundational fuel chemistry model to describe the oxidation of the pyrolysis products (Wang et al. 2007). The HyChem model consists of 119 species and 841 reactions. Additionally, the Princeton ozone submodel (Zhao et al. 2016) was incorporated into the HyChem model to perform calculations with ozone addition.

The governing equations for a one-dimensional detonation model are given in the literature elsewhere (Kumar et al. 2021). The induction zone length (Δ_i) and induction delay time (τ_i) were estimated by first calculating the detonation velocity, V_{CJ} for a particular initial condition. Von Neumann and CJ conditions of detonation wave are evaluated using SD Toolbox. The normal shock relations are used to evaluate the Von Neumann conditions like temperature T_{VN}, pressure P_{VN}, and density ρ_{VN}, which are then used as initial conditions for estimating the ZND structure by solving the conservation equations (Kumar and Singh 2021; Kumar et al. 2021). Further, Δ_i was evaluated as the distance from shock front to peak thermicity in the wave frame of reference. At the thermicity peak, (dT/dx) will be maximum. Similarly, the time scale from the leading shock front to thermicity peak represents the induction time (τ_i).

Results and Discussions

Computed Species Profiles for A1-, A2-, A3-air Mixtures

For each stoichiometric fuel–air mixture with A1, A2, and A3 as three different real fuels, ZND calculations were performed at 298 K and 1 atm to evaluate the detonation parameters. Behind the leading shock front, the high post-shock temperatures (~ 1500 K) facilitate the decomposition of the parent fuel molecule. The parent fuel molecule (A1, A2, and A3) undergoes pyrolysis first and gets decomposed into a set of key pyrolysis products. In this case, for all the three fuels studied, the key pyrolysis species are C_2H_4, H_2, C_3H_6, i-C_4H_8, CH_4, C_2H_6, 1-C_4H_8, C_7H_8, and C_6H_6 with C_2H_4 and CH_4 being the two most important species. The pyrolysis process does not require the presence of molecular oxygen and the slight decrease in oxygen concentration, as observed in Fig. 2, is due to molecular diffusion. From Fig. 2, it can be observed that for all the three fuels tested here (A1, A2, and A3), the concentration of key pyrolysis products are quite similar. This is because the composition of parent fuel molecule governs the distribution and concentration of pyrolysis products. The jet fuels considered here are quite similar in their chemical composition, where they contain different concentrations of n-paraffins, iso-paraffins, cyclo-paraffins, and aromatics. Therefore, during thermal decomposition or oxidative pyrolysis, they get decomposed into the same set of pyrolysis products and yield nearly the same amounts of pyrolysis products under comparable conditions. Following pyrolysis, the oxidation of decomposed products begins in the oxidation zone. Unlike the pyrolysis process, which is quite fast, oxidation is a slower step and is rate-limiting during the entire course of reaction leading to ignition. The rate of the oxidation of the pyrolysis products is critical to radical growth and heat release, and for this reason the composition of pyrolysis products determines the combustion and detonation properties of real distillate fuels. Evidently, by referring to Figs. 2 and 3, it can be observed that the length and time scales associated with the pyrolysis of parent fuel molecules are quite small when compared to the length and time scales associated with the oxidation of pyrolysis products. Since the oxidation of decomposed products is rate-limiting, a detailed reaction model is employed in HyChem to capture the oxidation process of pyrolysis products. The thermal decomposition process is not rate-limiting and hence can be modeled by 6–10 experimentally-constrained lumped reaction steps. The decomposition zone and the oxidation zone together constitute the induction zone for all real fuels. The line dividing

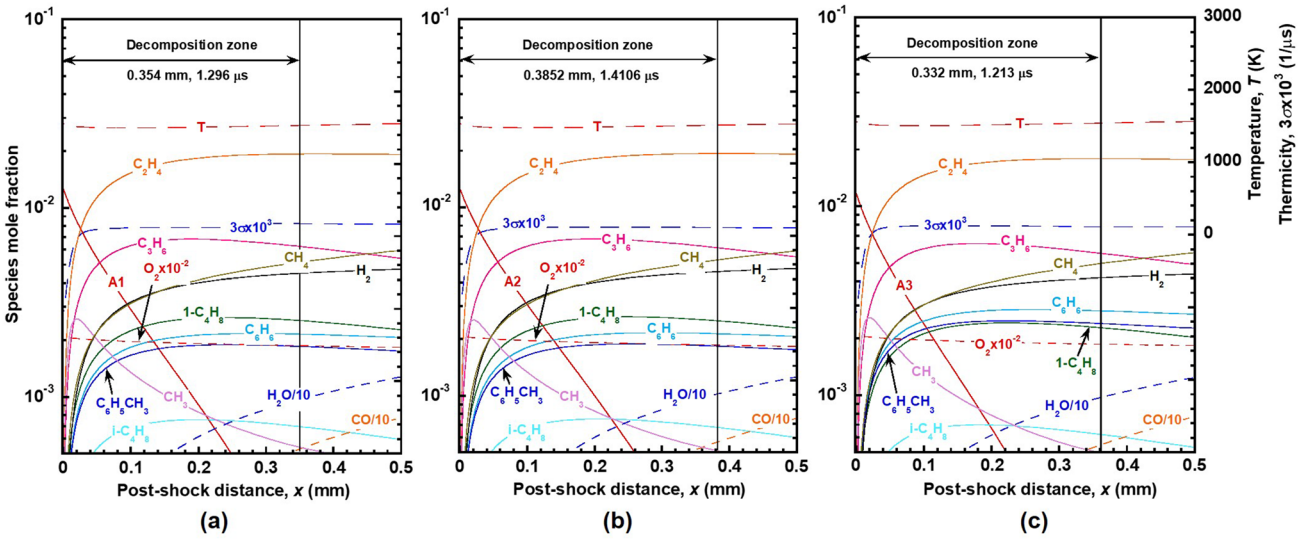

Fig. 2 Computed species profiles and representation of thermal decomposition zone for stoichiometric **a** A1–air, **b** A2–air, and **c** A3–air mixtures at $T_0 = 298$ K and $P_0 = 1$ atm

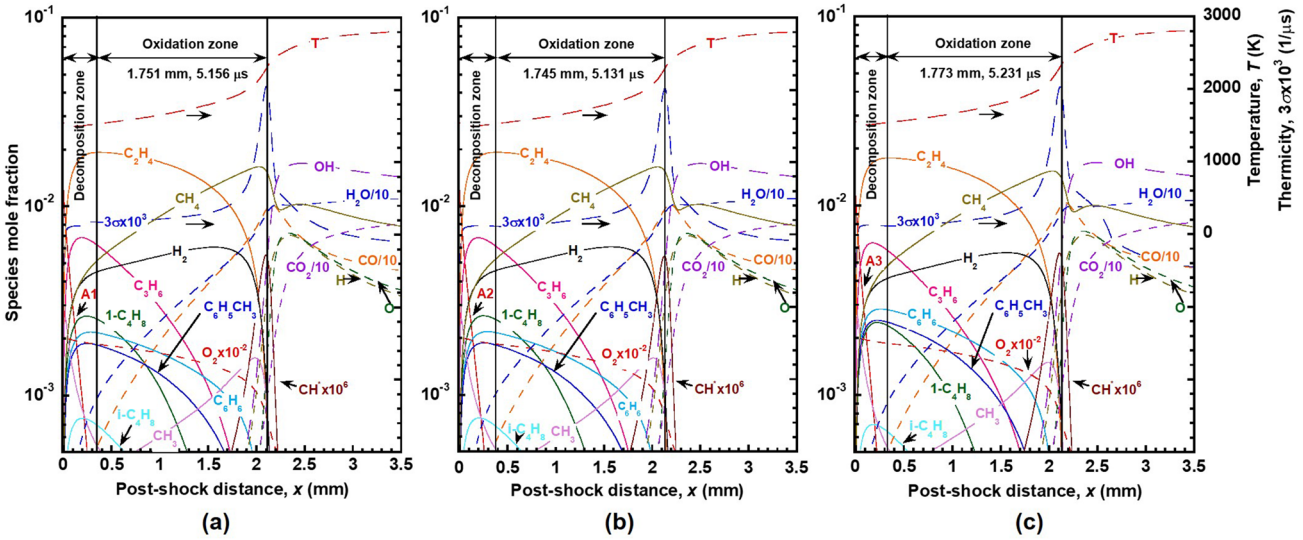

Fig. 3 Computed species profiles and representation of decomposition and oxidation zones for stoichiometric **a** A1–air, **b** A2–air, and **c** A3–air mixtures at $T_0 = 298$ K and $P_0 = 1$ atm

decomposition and oxidation is set at a value of 95% or more parent fuel disappearance. The oxidation zone follows the decomposition zone and represents the region that extends to the location of peak thermicity since major pyrolysis products are consumed within this region (see Figs. 2 and 3). Toward the end of the oxidation zone, the concentration of pyrolysis species rapidly drops, and the formation of CO_2, H_2O, and CO begins. Moreover, the maximum amount of energy from the chemicals bonds is converted to flow thermal energy at this location, as is evident from the peak in the thermicity curve (refer to Fig. 3). From Fig. 3, it can be observed that ethylene is the major pyrolysis species for all the three fuels investigated. This implies that the detonation chemistry of A1, A2, and A3 fuels are almost identical and the conventional jet fuels behave similarly in a detonating environment.

Also, the decomposition and oxidation zone length and time scales are approximately the same for the three real distillate fuels considered here. Overall, due to similar composition of pyrolysis products, the three jet fuels tested (A1, A2, and A3) indicate the same detonating behavior for a given initial condition. Additionally, the three jet fuels tested yield

nearly the same amounts of pyrolysis products under comparable conditions. This shows the insensitivity of the basic detonation responses to fuel composition since the pyrolysis product distribution determines the global combustion properties of the original, multicomponent real fuels. This observation supports the preconceived notion that when the number of components in a real distillate fuel is large enough, the rate behavior of the mixture exhibits diminishing sensitivity toward fuel composition and is in agreement with previous studies (Iyer and Singh 2022; Wang et al. 2018).

Effect of Equivalence Ratio

The calculation for varying equivalence ratios was evaluated for A1, A2, and A3 fuels at an initial pressure and temperature of 1 atm and 298 K, respectively. The variation of induction length and T_{CJ} with equivalence ratio is shown in Fig. 4a, whereas Fig. 4b shows the variation of induction time with equivalence ratio. For slightly rich mixtures (φ =1.1), the values of T_{CJ} are observed to be maximum. This is due to the large energy release at an equivalence ratio of 1.1. Similarly, the P_{CJ} and V_{CJ} exhibit a maximum around $\varphi = 1.1$. V_{CJ} primarily depends on the normalized energy content of the reactive mixture and is a property of the energetic gas. The equivalence ratio is observed to have a significant impact on the detonation parameters (refer to Fig. 4a and b). The induction time and length are found to be minimum near stoichiometric conditions (minimum occurs at φ = 1.1). Lower induction length and time scales represent mixtures that are more detonable and are indicative of robust detonations that have a strong coupling between the reaction zone and the leading shock front. However, for the fuel-lean and -rich mixtures, the length and time scales increase considerably, which indicates a loosely coupled

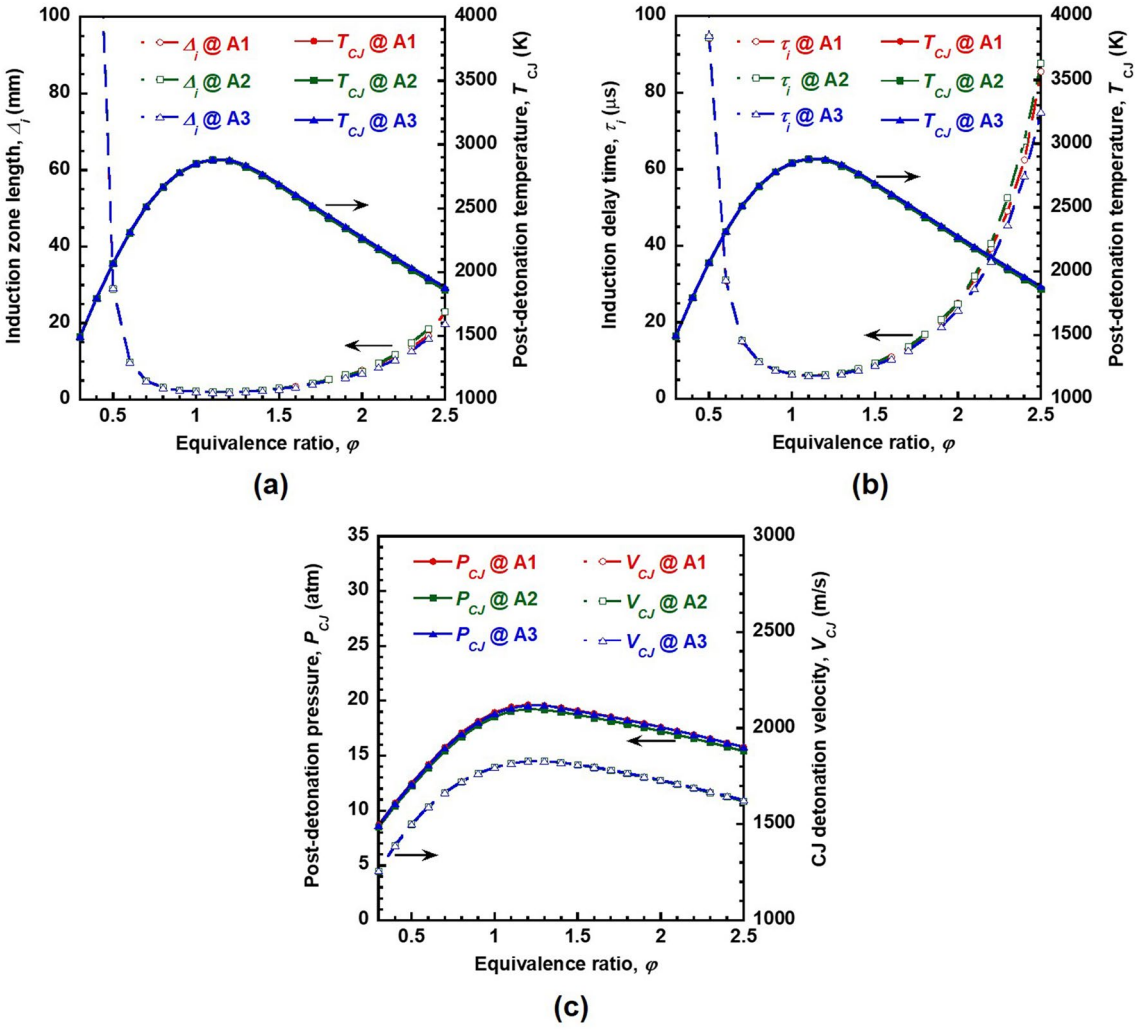

Fig. 4 Effect of equivalence ratio on detonation parameters of A1–, A2–, and A3–air mixtures, **a** induction length and T_{CJ}, **b** induction time and T_{CJ}, and **c** V_{CJ} and post-detonation pressure P_{CJ} at T_0 = 298 K and P_0 = 1 atm

shock flame complex and represents mixtures that are less detonable. Also, for these mixtures, the heat release is small when compared to the stoichiometric mixtures, thus leading to smaller T_{CJ} values. From Fig. 4a and b, it is to be noted that both the induction length and time scales and T_{CJ} seem to be similar for the three jet fuels considered in this study. Figure 4c indicates that the values of P_{CJ} and V_{CJ} also remain the same among all three conventional jet fuels. Typically the values only differ by small amounts and seem to coincide graphically. This is expected as the real distillate fuels considered in the given study have a large number of components which makes the rate behavior of the mixture exhibit small sensitivity toward fuel composition regardless of what components are found in the mixture. This explains the small sensitivity of detonation parameters to fuel composition variations and the same can be observed in Fig. 4. The equivalence ratio has a significant effect on the detonation parameters for a given fuel–air mixture. Comparing the effects of equivalence ratio on detonation parameters for A1, A2, and A3 fuels suggests that the trend for each parameter is almost identical for the conventional jet fuels considered in this study. It is observed that the influence of the equivalence ratio on the length and time scales and the post-detonation thermodynamic parameters is almost the same for the real distillate fuels considered in this study. Therefore, the performance of detonation-based engines is expected to have a small sensitivity to fuel composition variations if the number of components in a fuel mixture becomes large enough (> 12–14). Since conventional jet fuels considered in this study are multi-component distillate fuels and contain hundreds to thousands of chemical compounds they exhibit similar detonating characteristics over a range of equivalence ratios. Thus, the detonation chemistry and combustion properties of real distillate fuels (JP-8, Jet-A, and JP-5) are governed primarily by the composition of their key pyrolysis products rather than the details of the initial fuel composition, since these details are washed out if the number of components is large enough. Thus, in a fuel mixture in which the H/C ratio falls within a certain range and the number of components is large enough, the pyrolysis product distribution and detonation properties appear to vary little. The notion is supported through ZND computations for real distillate fuels at varying initial conditions and is discussed in the subsequent sections that follow. Table 2 presents the A1-air detonation parameters with varying equivalence ratio.

Effect of Initial Pressure and Temperature

The effect of varying initial pressure and temperature on the detonation parameters is presented in this section. The calculations for varying initial pressure are evaluated for the stoichiometric fuel–air mixtures at a fixed initial temperature of 298 K. The induction zone is dominated by two-body binary collisions. With the increase in initial pressure, the likelihood of these collisions is significantly increased, and this also increases the kinetic rate of chemical reactions that occur in the induction zone. As the chemical kinetics become faster, this leads to smaller induction length and time scales as observed in Fig. 5a. From Fig. 5b, a drastic increase in the P_{CJ} can be noted; however, the increase in T_{CJ} and M_{CJ} is not so profound with increasing initial pressures. Also, the CJ detonation velocity remains almost the same with increasing initial pressure (refer to Table 3). Similar to the previous case of varying equivalence ratios, initial pressure is observed to have a similar influence on the A1, A2, and A3 fuels. Real distillate fuels considered in this study exhibit almost identical trends with varying initial pressure and the same is depicted in Fig. 5a, and b. Table 3 presents the detonation parameters for A1-air detonations with varying initial pressure (P_0).

For the case of varying initial temperature, the ZND calculations were performed for stoichiometric mixtures at a fixed initial pressure of 1 atm. At higher initial temperatures,

Table 2 A1–air detonation parameters with varying equivalence ratio at $P_0 = 1$ atm and $T_0 = 298$ K. Values for A2- and A3-air detonations are not shown as they are very similar to that of A1-air detonations

φ	P_{VN} (atm)	T_{VN} (K)	M_{CJ}	V_{CJ} (m/s)	P_{CJ} (atm)	T_{CJ} (K)	Δ_i (mm)	τ_i (μs)
0.4	19.6	1119.2	4.1	1389.1	10.7	1794.3	148.0	484.2
0.5	23.1	1237.6	4.4	1499.6	12.5	2066.7	28.9	94.1
0.6	26.2	1337.6	4.7	1591.2	14.2	2308.9	9.7	30.9
0.7	29.0	1418.0	4.9	1664.8	15.7	2511.1	16.2	29.4
0.8	31.3	1478.8	5.1	1721.8	17.1	2666.9	3.2	9.7
0.9	33.2	1522.7	5.3	1764.8	18.1	2777.7	2.4	7.5
1	34.7	1552.3	5.4	1796.5	18.9	2848.6	2.1	6.5
1.1	35.8	1568.9	5.5	1817.8	19.5	2880.9	2.0	6.1
1.2	36.5	1572.2	5.5	1828.4	19.7	2873.0	6.7	11.5
1.3	36.8	1562.7	5.6	1828.8	19.6	2827.6	2.2	6.7
1.4	36.7	1544.4	5.6	1821.6	19.4	2758.4	2.5	7.7
1.5	36.5	1521.3	5.6	1810.2	19.1	2678.2	2.9	9.1

from the normal shock relations, the post-shock temperature (T_{VN}) increases drastically. As the chemical reactions in the induction zone are dependent on T_{VN} (from the Arrhenius equation), higher values of post-shock temperature lead to faster kinetic rates. This ultimately results in the smaller induction length and time scales at higher initial temperatures, as observed in Fig. 6a and Table 4. Also, at higher initial temperatures, the post-detonation temperature (T_{CJ})

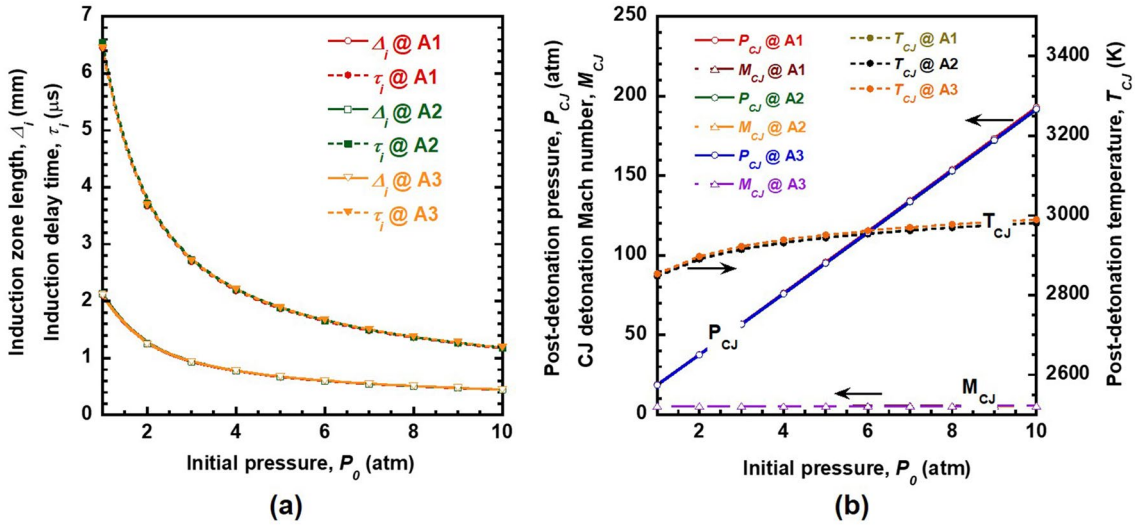

Fig. 5 Effect of initial pressure on **a** induction length and time, and **b** M_{CJ} and post-detonation thermodynamic parameters for A1–, A2–, and A3–air stoichiometric mixtures at $T_0 = 298$ K and $P_0 = 1$ atm

Table 3 A1–air detonation parameters with varying initial pressure (P_0) at $\varphi = 1$ and $T_0 = 298$ K. Values for A2- and A3-air detonations are not shown as they are very similar to that of A1-air detonations

P_0 (atm)	P_{VN} (atm)	T_{VN} (K)	M_{CJ}	V_{CJ} (m/s)	P_{CJ} (atm)	T_{CJ} (K)	Δ_i (mm)	τ_i (μs)
1	34.7	1552.3	5.4	1796.5	18.7	2848.6	2.1	6.5
2	70.3	1567.6	5.4	1808.6	37.8	2891.6	1.2	3.7
3	106.3	1576.1	5.5	1815.3	57.0	2915.8	0.9	2.7
4	142.4	1582.0	5.5	1819.9	76.3	2932.4	0.8	2.2
5	178.7	1586.4	5.5	1823.4	95.6	2945.0	0.7	1.9
6	215.2	1590.0	5.5	1826.2	115.0	2955.1	0.6	1.6
7	251.7	1592.9	5.5	1828.5	134.4	2963.4	0.5	1.5
8	288.3	1595.4	5.5	1830.4	153.9	2970.6	0.5	1.4
9	324.9	1597.6	5.5	1832.1	173.4	2976.8	0.5	1.3
10	361.6	1599.5	5.5	1833.6	192.8	2982.3	0.4	1.2

Table 4 A1–air detonation parameters with varying initial temperature (T_0) at $\varphi = 1$ and $P_0 = 1$ atm. Values for A2- and A3-air detonations are not shown as they are very similar to that of A1-air detonations

T_0 (K)	P_{VN} (atm)	T_{VN} (K)	M_{CJ}	V_{CJ} (m/s)	P_{CJ} (atm)	T_{CJ} (K)	Δ_i (mm)	τ_i (μs)
300	34.4	1553.6	5.4	1796.3	18.6	2848.8	2.1	6.4
400	25.7	1616.9	4.7	1789.1	14.0	2865.2	1.9	5.8
500	20.4	1683.5	4.2	1782.7	11.2	2884.5	1.7	4.9
600	16.9	1753.1	3.8	1777.0	9.4	2905.7	1.4	3.9
700	14.5	1825.5	3.6	1771.9	8.1	2928.2	1.1	3.0
800	12.6	1900.3	3.3	1767.1	7.1	2951.7	0.9	2.2
900	11.1	1977.5	3.1	1762.7	6.3	2975.8	0.7	1.6
1000	10.0	2056.8	3.0	1758.5	5.7	3000.5	0.5	1.2
1100	9.0	2137.6	2.9	1754.4	5.2	3025.2	0.4	0.9
1200	8.2	2219.4	2.7	1750.4	4.8	3050.0	0.3	0.7

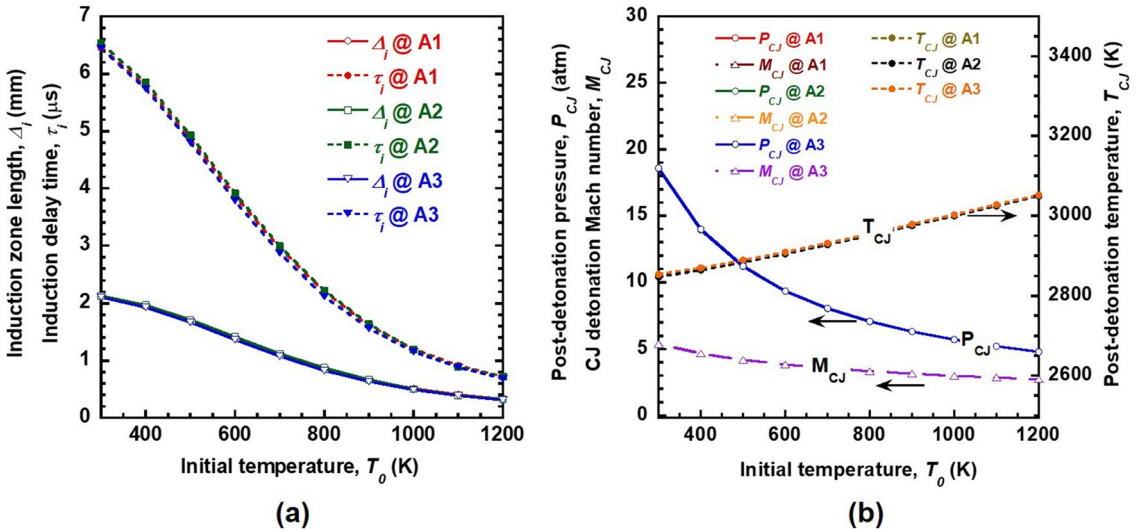

Fig. 6 Effect of initial temperature on **a** induction length and time scales, and **b** M_{CJ} and post-detonation thermodynamic parameters for stoichiometric A1–, A2–, and A3–air mixtures at $P_0 = 1$ atm

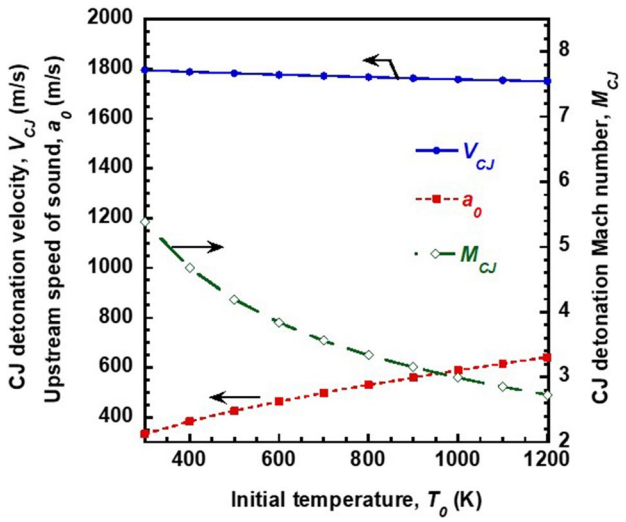

Fig. 7 Effect of initial temperature on gas dynamic properties (CJ detonation Mach number, CJ detonation velocity, and upstream speed of sound) for stoichiometric A1–air mixture at $P_0 = 1$ atm

increases (~2800–3000 K). However, a decrease in P_{CJ} and M_{CJ} can be observed with increasing initial temperatures (see Fig. 6b and Table 4). This is because the upstream speed of sound in the pre-shock unburnt mixture (a_0) before the incident shock greatly increases (owing to large values of T_0); however, V_{CJ} remains fairly the same (see Fig. 7). This leads to the decreasing values of M_{CJ} ($M_{CJ} = V_{CJ}/a_0$). Also, as the detonation Mach number reduces, it results in lower values of post-shock pressure (P_{VN}) as the initial pressure (P_0) is fixed in these calculations. Hence, with the lower values of P_{VN}, the post-detonation pressure (P_{CJ}) reduces and becomes much smaller than P_{VN} due to flow expansion in the reaction zone. A similar explanation can be extended to the post-shock density and post-detonation density (not shown in the figure). Table 4 presents the detonation parameters for A1-air detonations with varying initial temperature (T_0).

As observed in the case of initial pressure, the varying initial temperature seems to have a significant impact on the detonation parameters of A1–, A2–, and A3–air detonations. However, the trends exhibited by various parameters with varying initial temperature are almost identical for the three jet fuels considered in this study. It indicates that the initial thermodynamic parameters (varying initial temperature or initial pressure) affect the detonating behavior of A1, A2, and A3 fuels similarly. However, for a given fuel–air mixture, initial conditions significantly affect the length and time scales and post-detonation thermodynamic parameters.

Effect of Inert Diluents

The dilution effects of compounds, such as CO_2, H_2O, N_2, Ar, and He, on the gaseous detonations have been investigated previously (Kumar and Singh 2021; Kumar et al. 2021). However, in the present analysis, the effect of inert diluents on A1–, A2–, and A3–air detonating mixtures is considered. Inert diluents like argon and helium do not participate in chemical reactions and have a strictly thermal inhibiting effect on the detonation structure. Hence, only Ar and He are considered here. ZND calculations were performed for stoichiometric fuel–air-diluent mixtures at initial temperature and pressure of 298 K and 1 atm, respectively.

Figure 8a, b show the variation of induction length and time, respectively, with varying dilution levels of argon and helium. Since both the diluents are inert, they do not participate in chemical reactions; however, they do induce a strictly thermal inhibiting effect. This leads to an overall reduction in the exothermicity of the reactive mixture. The drastic reduction in the post-detonation temperature T_{CJ} can be attributed to this. Thus, for a given fuel–air-diluent mixture, post-detonation temperatures can be reduced at high dilution levels of argon and helium. From the perspective of engines working on detonation mode of combustion, the high temperatures in the combustion chamber could be controlled by diluting a given fuel–air mixture with inert diluents. Thus, high dilution levels can reduce the operating temperatures of a detonation-based engine.

The advantage of lowering the post-detonation temperatures (T_{CJ}) at high dilution levels comes at the cost of a reduced likelihood of detonation. This is evident from Fig. 8a, b and Table 5, where both the induction length and times continuously increase with increasing diluent concentration. It must be noted that T_{CJ} remains the same for a given dilution level for both argon and helium. Thus, thermal inhibition by argon and helium dilution is almost the same for real distillate fuels considered in this study. However, induction length and time scales increase considerably for helium dilution when compared to argon dilution. Thus, argon seems to be a better diluent than helium as for the same dilution levels it leads to a comparatively smaller increase in induction length and time scales while maintaining the same post-detonation temperature. Also, the

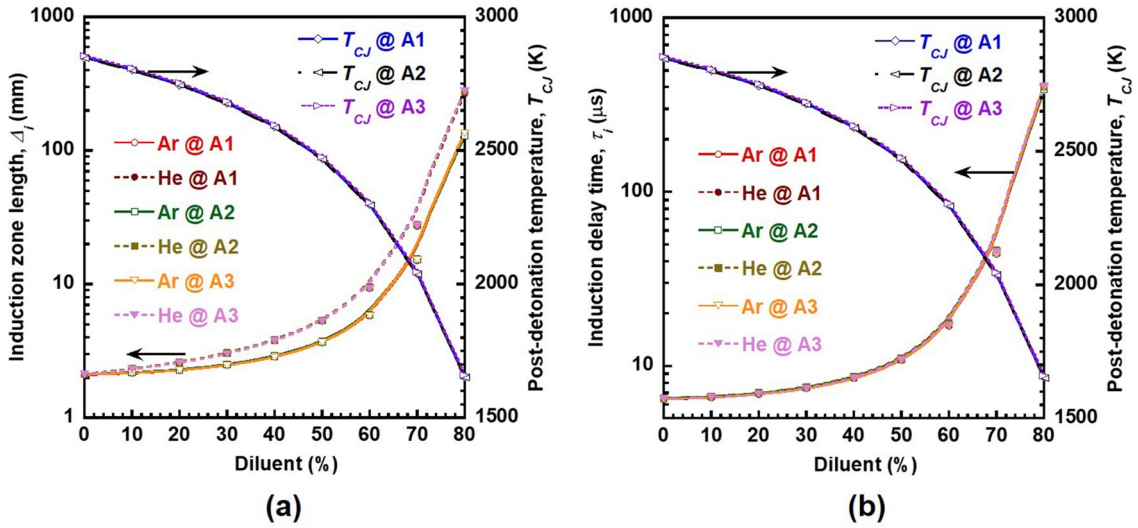

Fig. 8 Effect of the addition of inert diluents on **a** induction length and T_{CJ}, and **b** induction time and T_{CJ} for A1–, A2–, and A3–air stoichiometric mixtures at $T_0 = 298$ K and $P_0 = 1$ atm

Table 5 A1–air detonation parameters with varying concentration of inert diluents (molar-based %) at $P_0 = 1$ atm, $T_0 = 298$ K, and $\varphi = 1$. Values for A2- and A3-air detonations are not shown as they are very similar to that of A1-air detonations

X_{Fuel}	X_{Ox}	X_{Ar} (%)	X_{He} (%)	P_{VN} (atm)	T_{VN} (K)	M_{CJ}	V_{CJ} (m/s)	P_{CJ} (atm)	T_{CJ} (K)	Δ_i (mm)	τ_i (μs)
0.0126	0.9874	0	0	34.4	1553.6	5.4	1796.3	18.6	2848.8	2.1	6.4
0.0113	0.8887	10	0	33.3	1574.5	5.3	1746.0	18.0	2803.0	2.2	6.6
0.0101	0.7899	20	0	32.1	1593.8	5.2	1694.6	17.4	2747.7	2.3	6.9
0.0088	0.6912	30	0	30.6	1609.8	5.0	1641.2	16.7	2679.0	2.5	7.4
0.0075	0.5925	40	0	29.0	1619.0	4.9	1583.7	15.8	2590.4	2.9	8.5
0.0063	0.4937	50	0	27.1	1615.0	4.7	1518.8	14.7	2470.6	3.7	10.8
0.0113	0.8887	0	10	33.3	1574.5	5.3	1855.5	18.0	2803.0	2.3	6.6
0.0101	0.7899	0	20	32.1	1593.8	5.2	1921.7	17.4	2747.7	2.6	6.9
0.0088	0.6912	0	30	30.6	1609.8	5.0	1996.1	16.7	2679.0	3.0	7.5
0.0075	0.5925	0	40	29.0	1619.0	4.9	2079.4	15.8	2590.4	3.8	8.5
0.0063	0.4937	0	50	27.1	1615.0	4.7	2171.4	14.7	2470.7	5.3	10.9

real distillate fuels considered in this study behave similarly when inert diluents are added to fuel–air mixtures (refer to Fig. 8a, b). There is no notable difference in the detonation parameters when A1–, A2– and A3–air mixtures are diluted with argon or helium and the same is evident from Fig. 8a, b. Table 5 presents the detonation parameters for A1-air detonations with varying concentration of inert diluents.

Effect of Ignition Promoters

The effect of the addition of ignition promoters on A1–, A2– and A3–air detonating mixtures is evaluated and compared next for conventional jet fuels. ZND computations were computed for stoichiometric fuel–air mixtures at the initial condition of 1 atm and 298 K. The fuel–air mixtures were doped with varying concentrations of ozone and hydrogen peroxide and their effect on the chemical length and time scales was evaluated for a ZND detonation structure. Due to the addition of O_3 and H_2O_2, the induction length and time scales are observed to decrease continuously (refer to Fig. 9a, b). Ozone and hydrogen peroxide readily decompose into O and OH radicals respectively via the following reactions: $O_3 + M \rightarrow O_2 + O + M$ and $H_2O_2 + M \rightarrow 2OH + M$. The proliferation of O and OH radicals in the case of ozone and hydrogen peroxide accelerates the chain-branching process and shortens the induction delay time, τ_i. As the concentration of O and OH radicals increase, it fastens the ignition kinetics of detonating mixtures and results in a faster detonation process. Thus, the induction length and times are observed to decrease as the concentration of dopants or ignition promoters increases in a given fuel–air mixture. Similarly, the detonability of a given fuel–air mixture can be increased with the addition of ozone and hydrogen peroxide in trace amounts. It is observed that the post-detonation temperature T_{CJ} remains reasonably constant at small dopant levels of ozone and hydrogen peroxide and this is evident from Fig. 9a, b. This is also true for P_{CJ} and other post-shock thermodynamic parameters (P_{VN}, T_{VN}, etc.). This implies that both ozone and hydrogen peroxide only interfere with the chemical kinetics without affecting the post-shock and post-detonation thermodynamic parameters (refer to Fig. 9 and Table 6). Also, ozone and hydrogen peroxide when added in small concentrations do not affect the gas dynamic parameters, such as M_{CJ} and V_{CJ} (refer to Table 6). Thus, trace amounts of ignition promoters reduce the induction delay time of fuel–air mixtures significantly without affecting the thermodynamic and gas dynamic properties of the resulting mixture. This allows us to study the effect of chemistry in isolation. Table 6 presents the detonation parameters for A1-air detonations with varying concentration of ignition promoters.

A1, A2, and A3 fuels seem to have a similar likelihood of detonating upon the addition of ozone and hydrogen peroxide. The jet fuels considered in this study behave almost identically in the presence of ignition promoters and exhibit similar detonation characteristics. The detonation length and time scales and the post-detonation thermodynamic parameters are found to be almost the same for the real distillate fuels considered in this study.

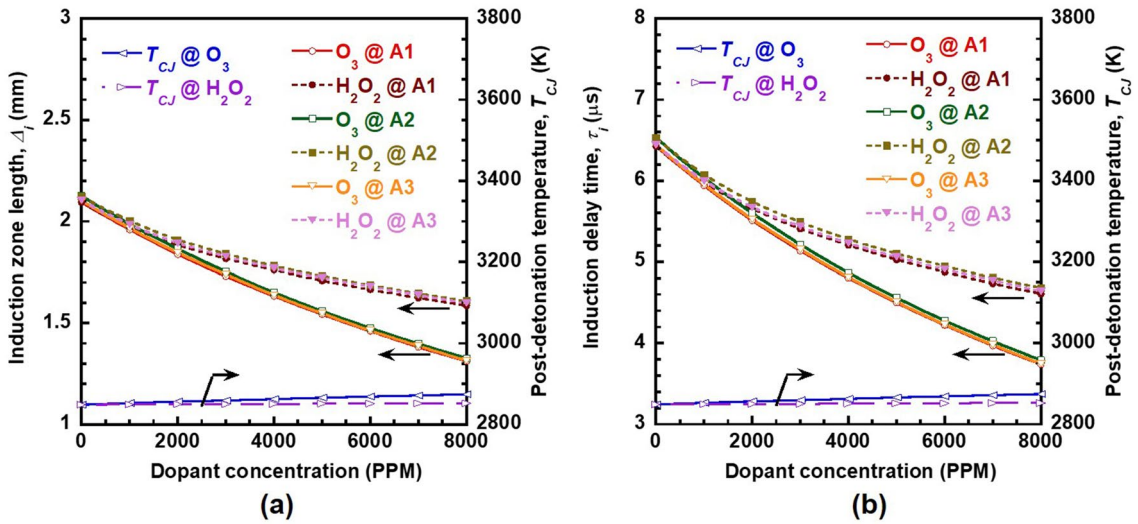

Fig. 9 Effect of varying concentration of ignition promoters on **a** induction length and T_{CJ}, and **b** induction time and T_{CJ} for A1–, A2–, and A3–air stoichiometric mixtures at $T_0 = 298$ K and $P_0 = 1$ atm

Table 6 Calculation of A1–air detonation parameters with varying concentration of ignition promoters (PPM-based) at $P_0 = 1$ atm, $T_0 = 298$ K, and $\varphi = 1$. Values for A2- and A3-air detonations are not shown as they are very similar to that of A1-air detonations

X_{O3} (PPM)	X_{H2O2} (PPM)	P_{VN} (atm)	T_{VN} (K)	M_{CJ}	V_{CJ} (m/s)	P_{CJ} (atm)	T_{CJ} (K)	Δ_i (mm)	τ_i (μs)
0	0	34.4	1553.6	5.4	1796.3	18.6	2848.8	2.1	6.4
1000	0	34.5	1555.0	5.4	1797.3	18.6	2852.6	2.0	5.9
2000	0	34.6	1556.4	5.4	1798.2	18.6	2856.2	1.8	5.5
3000	0	34.6	1557.7	5.4	1799.0	18.7	2859.6	1.7	5.1
4000	0	34.7	1559.0	5.4	1799.8	18.7	2862.8	1.6	4.8
5000	0	34.7	1560.2	5.4	1800.6	18.7	2866.0	1.5	4.5
0	1000	34.5	1553.6	5.4	1796.7	18.6	2849.4	2.0	6.0
0	2000	34.5	1553.6	5.4	1797.1	18.6	2849.9	1.9	5.7
0	3000	34.5	1553.6	5.4	1797.4	18.6	2850.4	1.8	5.4
0	4000	34.5	1553.6	5.4	1797.8	18.6	2850.8	1.8	5.2
0	5000	34.6	1553.5	5.4	1798.1	18.6	2851.3	1.7	5.0

Conclusions

In this study, detonation chemistry and critical detonation parameters have been computed using the ZND model for A1 (JP-8), A2 (Jet-A), and A3 (JP-5) fuels with air as the oxidizer. HyChem model was implemented to evaluate the detonation and ignition chemistry of real distillate fuels. The calculations were performed over a wide range of initial conditions. Specifically, the detonation parameters were evaluated for varying equivalence ratios, initial pressures, and initial temperatures. Over the range of conditions tested, the detonation chemistry and the values of critical detonation parameters were observed to be identical for A1, A2, and A3 fuels. The influence of inert diluents and ignition promoters on the detonation time and length scales and the post-detonation thermodynamic parameters were also evaluated. Similar to the case of initial conditions, the diluents and ignition promoters seem to affect the detonability of A1–, A2–, and A3–air mixtures, where the differences observed between three sets of fuel–air mixtures were small. Hence, for the test cases considered in this analysis, the three jet fuels indicate a similar possibility of detonation under comparable conditions. In so far as the global detonation properties are concerned, the three jet fuels tested exhibit nearly the same chemical behaviors and global detonation properties. This is because the rate behavior of the fuel–air mixture has a diminishing sensitivity toward fuel composition when the number of components in the mixture is large enough (> 12–14). Since conventional jet fuels considered in this study are multi-component distillate fuels and contain hundreds to thousands of chemical compounds, they exhibit similar detonating characteristics over a range of initial conditions. Therefore, the performance of detonation-based engines is expected to have a small sensitivity to fuel composition variations when the number of components in a fuel mixture becomes large enough. Thus, the global detonation properties of real distillate fuels (JP-8, Jet-A, and JP-5) are governed primarily by the composition of their key pyrolysis products rather than the details of the initial fuel composition, since these details are washed out if the number of components is large enough. Thus, in a fuel mixture in which the H/C ratio falls within a certain range and the number of components is large enough, the pyrolysis product distribution and detonation properties appear to vary little.

Acknowledgements The authors acknowledge the financial support for this work from the Aeronautics R&D Board, Ministry of Defence, Govt. of India vide Sanction Letter # ARDB/01/1042000M/I.

References

Browne S, Ziegler J, Shepherd JE (2008) Numerical solution methods for shock and detonation jump conditions. Galcit Rep fm2006 6:90

Crane J, Shi X, Singh AV, Tao Y, Wang H (2019) Isolating the effect of induction length on detonation structure: hydrogen-oxygen detonation promoted by ozone. Combust Flame 200:44–52. https://doi.org/10.1016/j.combustflame.2018.11.008

Dahake AP, Singh AV (2021) Numerical study on NO*x* emissions from a synthetic biofuel for applications in detonation-based combustors. In: AIAA propulsion and energy 2021 forum, p 3678. https://doi.org/10.2514/6.2021-3678

Dahake A, Singh AV (2022a) A comparative study of critical detonation parameters for jet A and an alcohol-to-jet synthetic biofuel. In: 2022a AIAA SciTech forum and exposition, 3–7 January 2022, San Diego, CA, USA. https://doi.org/10.2514/6.2022-0819

Dahake A, Singh AV (2022b) Effect of fuel sensitization on NO_x emissions from a synthetic biofuel under detonating conditions. In: 2022b AIAA SciTech forum and exposition, 3–7 January 2022, San Diego, CA, USA. https://doi.org/10.2514/6.2022-0518

Demirbas A (2008) Biofuels sources, biofuel policy, biofuel economy and global biofuel projections. Energy Convers Manage 49(8):2106–2116. https://doi.org/10.1016/j.enconman.2008.02.020

Garikov AI, Efimenko AA, Dorofeev SB (2000) A model for detonation cell size prediction from chemical kinetics. Combust Flame 120(1–2):19–33. https://doi.org/10.1016/S0010-2180(99)00076-0

Goodwin DG, Speth RL, Moffat HK, Weber BW (2018) Cantera: an object-oriented software toolkit for chemical kinetics, thermodynamics, and transport processes, version 2.4.0. https://www.cantera.org

Heiser WH, Pratt DT (2002) Thermodynamic cycle analysis of pulse detonation engines. J Propul Power 18(1):68–76. https://doi.org/10.2514/2.5899

Iyer KM, Singh AV (2021) NO*x* emissions from Jet A-air detonations. In: AIAA propulsion and energy 2021 forum, p 3679. https://doi.org/10.2514/6.2021-3679

Iyer MSK, Singh AV (2022) Ignition kinetics of real distillate fuels under detonating conditions. In: 2022 AIAA SciTech forum and exposition, 3-7 January 2022, San Diego, CA, USA. https://doi.org/10.2514/6.2022-0816

Kailasanath K (2000) Review of propulsion application of detonation waves. AIAA J 38(9):1698–1708. https://doi.org/10.2514/2.1156

Kao S, Shepherd JE (2008) Numerical solution methods for control volume explosions and ZND detonation structure. Galcit Rep fm2006 7:1–46

Kumar DS, Singh AV (2021) Inhibition of hydrogen-oxygen/air gaseous detonations using CF_3I, H_2O, and CO_2. Fire Saf J 124:103405. https://doi.org/10.1016/j.firesaf.2021.103405

Kumar DS, Ivin K, Singh AV (2021) Sensitizing gaseous detonations for hydrogen/ethylene-air mixtures using ozone and H_2O_2 as dopants for application in rotating detonation engines. Proc Combust Inst 38(03):3825–3834. https://doi.org/10.1016/j.proci.2020.08.061

Liang W, Wang Y, Law C (2019) Role of ozone doping in the explosion limits of hydrogen-oxygen mixtures: multiplicity and catalyticity. Combust Flame 205:7–10. https://doi.org/10.1016/j.combustflame.2019.03.038

Lu FK, Braun EM (2014) Rotating detonation wave propulsion: experimental challenges, modeling, and engine concepts. J Propul Power 30(5):1125–1142. https://doi.org/10.2514/1.B34802

Mevel R, Lafosse F, Catoire L, Chaumeix N, Dupre G, Paillard CE (2008) Induction delay times and detonation cell size prediction of hydrogen-nitrous oxide-diluent mixtures. Combust Sci Tech 180(10–11):1858–1875. https://doi.org/10.1080/00102200802261340

Nicholls JA, Cullen RE, Ragland KW (1966) Feasibility studies of a rotating detonation wave rocket motor. J Spacecr Rocket 3(6):893–898. https://doi.org/10.2514/3.28557

Peng H, Liu W, Liu S, Zhang H (2018) Experimental investigations on ethylene-air continuous rotating detonation wave in the hollow chamber with Laval nozzle. Acta Astronaut 151:137–145. https://doi.org/10.1016/j.actaastro.2018.06.025

Rodionova MV, Poudyal RS, Tiwari I, Voloshin RA, Zharmukhamedov SK, Nam HG, Zayadan BK, Bruce BD, Hou HJM, Allakhverdiev SI (2017) Biofuel production: challenges and opportunities. Int J Hydrogen Energy 42(12):8450–8461. https://doi.org/10.1016/j.ijhydene.2016.11.125

Stamps DW, Tieszen SR (1991) The influence of initial pressure and temperature on hydrogen-air-diluent detonations. Combust Flame 83(3–4):353–364. https://doi.org/10.1016/0010-2180(91)90082-M

Vasil'ev AA (2006) Cell size as the main geometric parameter of a multifront detonation wave. J Propulsion Power 22(6):1245–1260. https://doi.org/10.2514/1.20348

Wang H, Xu R, Wang K, Bowman CT, Davidson DF, Hanson RK, Brezinsky K, Egolfopoulos FN (2018) A physics-based approach to modeling real-fuel combustion chemistry—I. Evidence from experiments and thermodynamic, chemical kinetics, and statistical considerations. Combust Flame 193(01):502–519. https://doi.org/10.1016/j.combustflame.2018.03.019

Wang H, You X, Joshi AV, Davis SG, Laskin A, Egolfopoulos F, Law CK (2007) USC Mech Version II. High-temperature combustion reaction model of H_2/CO/C_1-C_4 compounds. http://ignis.usc.edu/Mechanisms/USC-Mech%20II/USC_Mech%20II.htm

Westbrook CK (1982) Chemical kinetics of hydrocarbon oxidation in gaseous detonations. Combust Flame 46:191–210. https://doi.org/10.1016/0010-2180(82)90015-3

Wolański P (2013) Detonative propulsion. Proc Combust Inst 34(1):125–158. https://doi.org/10.1016/j.proci.2012.10.005

Zhang B (2019) Detonation limits in methane-hydrogen-oxygen mixtures: dominant effect of induction length. Int J Hydrogen Energy 44(41):23532–23537. https://doi.org/10.1016/j.ijhydene.2019.07.053

Zhao H, Yang X, Ju Y (2016) Kinetic studies of ozone assisted low temperature oxidation of dimethyl ether in a flow reactor using molecular-beam mass spectrometry. Combust Flame 173:187–194